Seeking neutrino emission from AGN through temporal and spatial cross-correlation

Cyril Creque-Sarbinowski,[*] Marc Kamionkowski,[†] and Bei Zhou[‡]

Department of Physics and Astronomy, Johns Hopkins University, 3400 N. Charles Street, Baltimore, Maryland 21218, USA

(Received 19 November 2021; accepted 23 May 2022; published 29 June 2022)

Active galactic nuclei (AGN) are a promising source for high-energy astrophysical neutrinos (HEANs). In 2024, the Vera C. Rubin Observatory (Rubin) will begin to observe $\gtrsim 10$ million AGN with a regular and high cadence. Here, we evaluate the capacity of Rubin, in tandem with various current and upcoming neutrino telescopes, to establish AGN as HEAN emitters. To do so, we assume that the neutrino luminosity from any given AGN at any given time is proportional to the electromagnetic luminosity. We then estimate the error with which this fraction can be measured through spatial and temporal cross-correlation of Rubin light curves with IceCube, KM3NeT, and Bakail-GVD. We find that it may be possible to detect AGN contributions at the $\sim 3\sigma$ level to the HEAN flux even if these AGN contribute only $\sim 10\%$ of the HEAN flux. The bulk of this information comes from spatial correlations, although the temporal information improves the sensitivity a bit. The results also imply that if an angular correlation is detected with high signal-to-noise, there may be prospects to detect a correlation between AGN variability and neutrino arrival times. The small HEAN fraction estimated here to be accessible to the entirety of the Rubin AGN sample suggests that valuable information on the character of the emitting AGN may be obtained through similar analyses on different subpopulations of AGN.

DOI: 10.1103/PhysRevD.105.123035

I. INTRODUCTION

High-energy astrophysical neutrinos (HEANs) comprise a diffuse isotropic extragalactic background of neutrinos observed with energies between a few TeV to a few PeV [1–4]. There is some evidence of an association of some these neutrinos with the blazar TXS $0506+056$ [5,6], but the source of the vast majority of the HEAN background remains a mystery. Various classes of bright AGN population have been constrained to contribute no more than a fraction of the total observed HEAN flux [7–12], but there is little known about the possible contribution of the many lower-luminosity AGN. With the advent of the Vera Rubin Observatory in 2024, at least 10 million AGN will be observed in the southern sky with high cadence for the following 10 years [13]. In addition, neutrino telescopes KM3NeT and Baikal-GVD will soon be completed in the northern hemisphere with comparable volume and better angular resolution than IceCube [14,15]. Due to their locations, these telescopes will detect HEAN from upgoing tracks originating from the southern sky without contamination from the atmospheric neutrino background. Thus, over the next decade of AGN and neutrino observations, we expect a large increase in sensitivity in the determination of AGN as HEAN emitters.

AGN are hypothesized to emit high-energy neutrinos through either hadronuclear [16,17] or photohadronic [18,19] processes. Therefore, one avenue of examination is the modelling of these processes under various AGN environments. High-energy neutrinos can be produced from radio-quiet AGN [20–22], radio-loud AGN jets [23–25], blazar inner cores and jets [9,26], and AGN coronae [27–30]. They may also have nothing to do with AGN—e.g., they may be associated with choked supernova jets [31], tidal disruption events [32–35] and even cosmic strings [36,37]. Even without theoretical modeling, information about the source of neutrinos may be sought with the coincidence of neutrino events with various source events through data alone [11,12,38–47].

In this work we present a statistical framework to determine whether HEANs are produced by AGN and assess its potential in the context of Rubin, IceCube, KM3NeT, and Baikal-GVD. More specifically, we propose to cross-correlate temporal and spatial data from AGN variability and neutrino events. To evaluate the prospects to detect such a cross-correlation, we make the simplest assumption that the neutrino flux from any given AGN at any given time is proportional to the electromagnetic flux at that given time. We then use state-of-the-art information on the AGN redshift/luminosity distribution and variability parameters to forecast the detectability of this cross-correlation. We find, with the AGN population assumed, that a correlation can be established even if the AGN in

[*]creque@jhu.edu
[†]mkamion1@jhu.edu
[‡]beizhou@jhu.edu

Rubin contribute as little as a few percent to the HEAN flux. Most of the sensitivity comes from angular information; the temporal information contributes approximately 10% of the signal to noise. Our estimates suggest that the better angular resolution (∼0.2°) expected for Baikal-GVD and KM3NeT, relative to the ∼0.5° for IceCube, will give them roughly twice the sensitivity to an AGN-neutrino cross-correlation for equal exposure.

This paper is organized as follows. In Sec. II we present the formalism of the AGN/neutrino cross-correlation. We discuss our model for the AGN redshift/luminosity distribution and the variability properties of AGN in Sec. III. We provide and discuss numerical results in Sec. IV. We discuss these results and conclude in Secs. V and VI, respectively.

II. FORMALISM

Our aim will be to determine the fraction f of neutrinos that come from AGN in the sample under the hypothesis that the neutrino flux from any given AGN at any given time is proportional to the electromagnetic flux from that AGN at that given time. To begin, we will simplify by neglecting AGN variability and then generalize later.

A. Angular information only

The optimal estimator to determine the fraction f of neutrinos that come from AGN in the sample will be the unbinned maximum-likelihood estimator [12,48–51],

$$\mathcal{L}(f;\text{data}) = \Pi_i[fS_i + (1-f)B_i], \tag{1}$$

where the product is over all neutrino events. Here, $S_i = S(\vec{\theta}_i)d^2\vec{\theta}$ is the probability that a given source neutrino will be found in a differential area $d^2\theta$ centered at the position θ_i of the ith neutrino, and $B_i = B(\vec{\theta}_i)d^2\theta_i$ the analogous quantity for a background neutrino. We normalize both distributions such that their integral over the area $4\pi f_{\rm sky}$ of the survey (where $f_{\rm sky}$ is the fraction of the sky surveyed) is equal to 1. We assume that background events follow a uniform sky distribution, i.e., $B_i = (4\pi f_{\rm sky})^{-1}$, which we justify in Appendix. Finally, we take the signal probability to be

$$S_i = \sum_\alpha w_\alpha \frac{1}{2\pi\sigma^2}\exp\left(-\frac{(\vec{\theta}_i - \vec{\theta}_\alpha)^2}{2\sigma^2}\right). \tag{2}$$

The sum on α is over all AGN in the sample, $\vec{\theta}_\alpha$ is the position of the αth AGN, and σ is the error in the neutrino angular position. Here, w_α is the probability that a given signal neutrino comes from the αth AGN, and so $\sum_\alpha w_\alpha = 1$.

Even if there is no signal, the likelihood will most generally be maximized at a value of f selected from a distribution with a variance σ_f^2 determined from

$$\frac{1}{\sigma_f^2} = \left\langle \left(\frac{\partial \ln \mathcal{L}(f;\text{data})}{\partial f}\right)^2 \right\rangle, \tag{3}$$

where the derivative is evaluated at $f = 0$, and the average is taken over all realizations of the data under the null hypothesis. We use

$$\left(\frac{\partial \ln \mathcal{L}}{\partial f}\right)_{f=0} = \sum_i \left(\frac{S_i}{B} - 1\right). \tag{4}$$

We then evaluate the expectation value

$$\left\langle \left(\frac{S}{B} - 1\right)^2 \right\rangle = \frac{4f_{\rm sky}}{\sigma^2 N_{\rm AGN}} \frac{\langle w_\alpha^2\rangle}{\langle w_\alpha\rangle^2}, \tag{5}$$

from the zero-lag correlation function for a collection of $N_{\rm AGN}$ randomly distributed AGN. Here, the angle brackets denote an average over all AGN in the sample. Our hypothesis here is that the neutrino flux from AGN α is proportional to its electromagnetic F_α, and so the correlation of N_ν neutrinos with AGN can be established with a signal-to-noise,

$$\frac{S}{N} \simeq 2\frac{f}{\sigma}\sqrt{\frac{N_\nu}{N_{\rm AGN}}\frac{\langle F_\alpha^2\rangle}{\langle F_\alpha\rangle^2} f_{\rm sky}}. \tag{6}$$

The result has the expected scalings with $f_{\rm sky}$, σ, N_ν, and $N_{\rm AGN}$. That is, Eq. (6) depends on the ratio of the number of neutrinos to the number of AGN in a neutrino's angular-resolution bin $N_{\rm AGN}[(\pi\sigma^2)/(4\pi f_{\rm sky})]$. If this ratio is small, one neutrino spatially overlaps with so many AGN that it is hard to detect a signal even when all neutrinos are taken into account. The signal to noise is also weighted by the ratio $\langle F_\alpha^2\rangle/\langle F_\alpha\rangle^2$ of the second moment of the AGN flux distribution to the square of the first moment (i.e., average flux).

B. Including AGN variability

The derivation above can be easily generalized to include the additional information provided by cross-correlating the neutrino arrival times with AGN luminosity at any given time. If the neutrino luminosity at any given time is correlated with the AGN luminosity at that same time, then the probability to detect a neutrino when a given AGN is, say, twice as bright, should be twice as large, as illustrated in Fig. 1.

To incorporate this correlation into the likelihood analysis above, we simply assume that the flux F_α for any given AGN in the likelihood function is the apparent flux *at the neutrino arrival time*. The signal-to-noise contributed by each AGN is then enhanced by a factor,

$$\left[\frac{\langle F^2(t)\rangle}{\langle F(t)\rangle^2}\right]^{1/2}, \tag{7}$$

where here $\langle F(t)\rangle$ is the time-averaged flux and $\langle F^2(t)\rangle$ the time-averaged squared flux. Thus, for example, if an AGN has a sinusoidal flux variation, $F(t) = F_0 + F_1\cos\omega t$, the

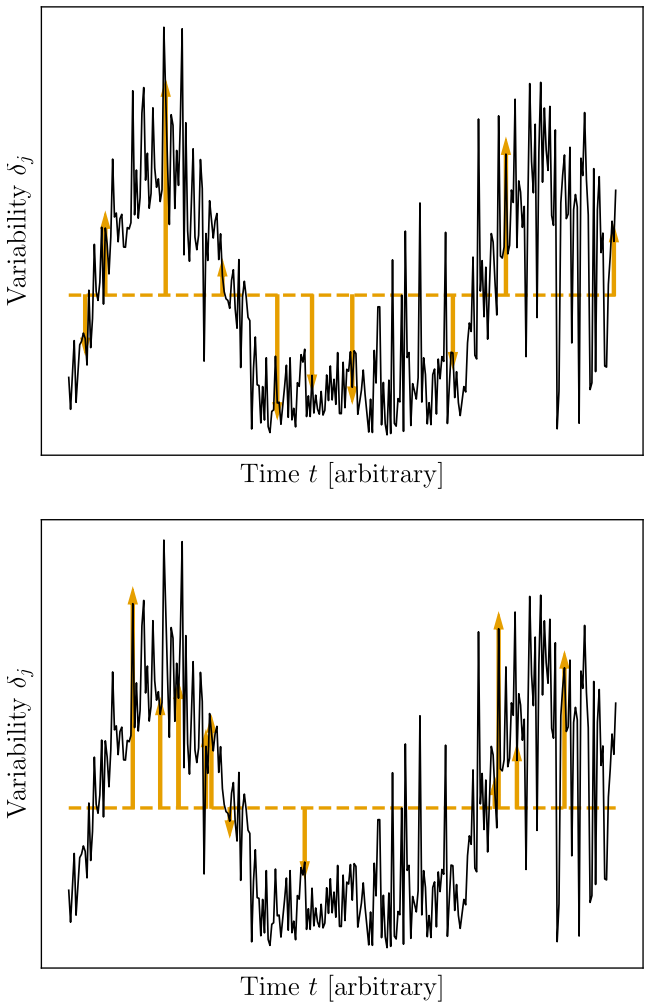

FIG. 1. An example of the variability $\delta_j(t)$ of AGN j shown in solid black, plotted against the variability $\delta_j(t_\alpha)$ evaluated at the neutrino arrival times t_α, depicted by solid orange arrows. The dashed orange line indicates the zero point, $\delta_j = 0$. In the top figure the neutrinos arrive randomly, and thus a cross-correlation between these two quantities would become zero. In the bottom figure the neutrinos are sourced from AGN and thus are biased towards appearing when the intensity is higher, leading to nonzero correlation.

contribution of this AGN to the total signal-to-noise is enhanced by a factor $[1 + (F_1/F_0)/2]^{1/2}$.

Of course, AGN variability is complicated and poorly understood. Below we describe a model for AGN variability but here note that the signal-to-noise with which f can be inferred will be enhanced by a factor $[1 + \langle\sigma^2_{\rm var}\rangle/2]^{1/2}$, where $\langle\sigma^2_{\rm var}\rangle$ is an appropriately weight rms fractional flux variation.

III. THE AGN POPULATION

A. The flux distribution

Here we model the flux distribution we expect for AGN in Rubin. Let $dN_{\rm AGN}/dzdL$ be the redshift and bolometric luminosity distribution of AGN. Then AGN are distributed throughout the Universe according to

$$\frac{dN_{\rm AGN}(z,L)}{dzdL} = \frac{dV(z)}{dz}\frac{dn(z,L)}{dL}, \tag{8}$$

with $dn(z,L)/dL$ the AGN luminosity function, $dV(z)/dz = 4\pi f_{\rm sky} r(z)^2 dr(z)/dz$ the comoving volume observed over a fraction $f_{\rm sky}$ of the sky, $r(z) = \int_0^z |dr/dz|dz$ the comoving radial distance to a redshift z, $dr/dz = -c/(1+z)H(z)$ its redshift derivative, c the speed of light, and $H^2(z) = H_0^2[\Omega_m(1+z)^3 + (1-\Omega_m)]^{-1/2}$ the Hubble parameter. We use Planck 2018 ΛCDM parameters $H_0 = 2.18 \times 10^{-18}$ s^{-1} and $\Omega_m = 0.315$ [52], along with the full AGN luminosity function in Table 3 from Ref. [53].

However, given a cosmological distribution of AGN, only those that appear bright enough will be observed. More specifically, given a limiting apparent magnitude $m_{\rm lim}$, the distribution of observed AGN in that band is

$$\frac{dN_{\rm AGN}}{dzdm} = \Theta(m_{\rm lim} - m)\frac{dL_{\rm bol}}{dm}\frac{dN_{\rm AGN}[z, L_{\rm bol}(z,m_b)]}{dzdL_{\rm bol}}, \tag{9}$$

with $\Theta(x)$ the Heaviside theta function, $L_{\rm bol}(z,m) = K_o(m)4\pi d_L(z)^2\langle\delta\nu_b\rangle F_{\rm AB} 10^{-(2/5)m_b}$ the bolometric luminosity for an AGN with apparent magnitude m averaged over frequency bands b located at redshift z, and $dL_{\rm bol}/dm = -(2/5)\log(10)L_{\rm bol}(m,z)$ its apparent magnitude derivative. Furthermore, $K_o(m)$ is the bolometric correction function to convert from the emitted luminosity in the optical band to the bolometric luminosity of the source, $d_L(z) = (1+z)r(z)$ the luminosity distance, $\delta\nu_b$ the frequency bandwidth of band b, and $F_{\rm AB} = 3.631 \times 10^{-23}$ W Hz^{-1} m^{-2}. Moreover, we assume that the observed intensity is roughly constant across the entire

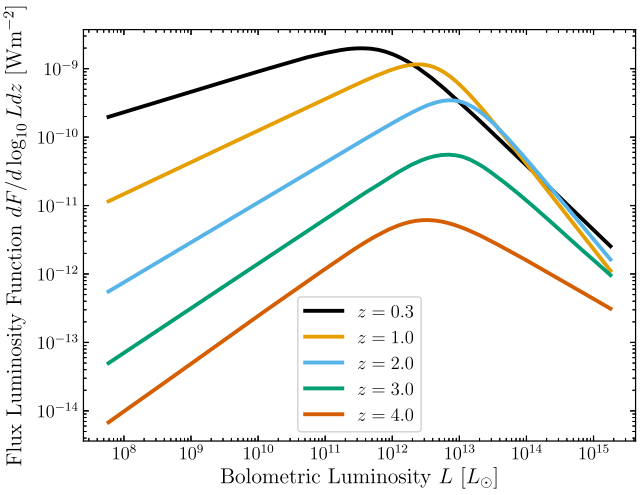

FIG. 2. The flux distribution of AGN as a function of an AGN's bolometric luminosity at redshifts $z \in \{0.3, 1.0, 2.0, 3.0, 4.0\}$, as given by Eq. (8).

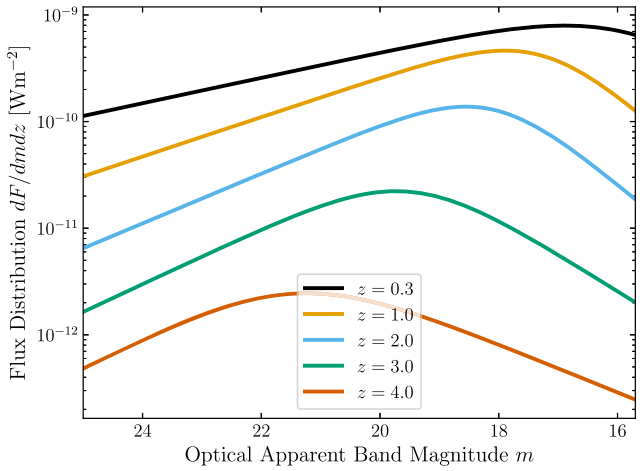

FIG. 3. The flux distribution of AGN as a function of an AGN's apparent magnitude in an optical band b at redshifts $z \in \{0.3, 1.0, 2.0, 3.0, 4.0\}$, as given by Eq. (9). In order to show the full range of this distribution, we do not include the theta function factor.

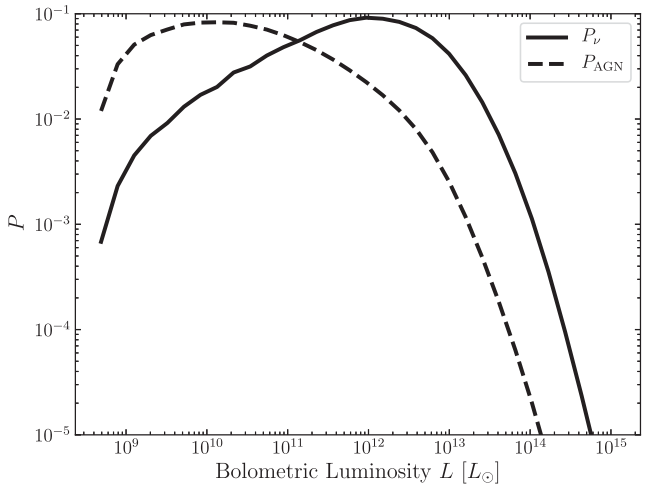

FIG. 4. The observation probability P associated with neutrinos and AGN in each bolometric luminosity bin between redshifts $0.3 \leq z \leq 6.7$. Over the range of luminosities presented, 33 base-10 logarithmic bins are taken. The solid black line is the probability that an AGN emitting neutrinos has bolometric luminosity L, while the dashed black line is the probability of that an observed AGN has bolometric luminosity L. Both curves are normalized by the set of observed AGN and are computed assuming a limiting magnitude of $m_{\rm lim} = 24.0$. At large luminosities both curves follow the expected flux distribution curve of Fig. 2, however at small L the limiting magnitude restricts the total number of AGN observed.

frequency bandwidth, and that any redshifting effects on the frequency do not alter the intensity in each band significantly. While the bolometric correction is typically a function of the apparent magnitude, it only varies up to 20% within the optical band across the magnitudes considered. Thus, for simplicity, we adopt that $K_o(m) = 10$ for all magnitudes and bands [53].

We define $dF_{\rm AGN}/dzdL$ to be the AGN flux luminosity distribution, and $dF^b_{\rm AGN}/dzdm \equiv FdN^b_{\rm AGN}/dzdm$ its magnitude counterpart. We plot the flux luminosity distribution in Fig. 2 and the magnitude distribution in Fig. 3.

In Fig 4 we plot the bolometric-luminosity distribution of AGN in the forecast Rubin sample and also the bolometric-luminosity weighted by the luminosity—this latter quantity is then proportional to the probability, under our assumptions, that a given neutrino comes from an AGN of some given luminosity.

B. AGN variability

The study of AGN variability is in its infancy when compared to how it will appear in the Rubin era [54]. We thus have far less in the way of precise current knowledge to make forecasts for the possibility to detect the cross-correlation between AGN variability and neutrino arrival times. To do so, though, we assume AGN light curves undergo a damped random walk [55–63], a model that provides a reasonable description of most light curves. In this case, the intensity $I_\alpha(t)$ of AGN α undergoes fluctuations described by a stationary random process with two-point correlation function, $\langle I_\alpha(t+t')I_\alpha(t)\rangle = A^2_\alpha e^{-t/\bar{t}_\alpha}$, or equivalently, a power spectrum $P_\alpha(\omega) = 2A^2_\alpha \bar{t}_\alpha/[1+(\omega\bar{t}_\alpha)^2]$. We assume that AGN all have the same variability amplitude $A_\alpha = 1$ and an observer-frame variability timescale $\bar{t}_\alpha = \bar{t}_0(1+z)\times(L/L_b)^\beta$ for an AGN of luminosity L at redshift z, as suggested by recent measurements [63]. We take $\bar{t}_0 =$ 1 month, $L_b = 2\times 10^{35}$ W, and $\beta = 0.23$. Our calculation then discards Fourier modes with periods longer or shorter than those accessed by Rubin.

Given this population of AGN, we can write the fractional flux variation as

$$\sigma^2_{\rm var} = \frac{1}{\pi}\frac{1}{\langle F^2_\alpha\rangle}\int_{\omega_{\rm min}}^{\omega_{\rm max}} d\omega \langle F^2_\alpha P_\alpha(\omega)\rangle, \tag{10}$$

where only modes between $\omega_{\rm min} = 2\pi/T$ and $\omega_{\rm max} = 2\pi/\Delta t$ are included, with $\Delta t = 3.5$ days the temporal resolution of the experiment and $T = 10$ years the duration of the observation.

IV. FORECASTS

We now forecast the ability of the neutrino telescopes IceCube, KM3NeT, and Baikal-GVD, along with optical telescope Rubin, to determine the fraction f of neutrinos that come from AGN in the survey.

A. Angular information only

With our model for the AGN luminosity/redshift distribution and Rubin's apparent-magnitude cutoff, we forecast

$N_{\rm AGN} \simeq 2.8 \times 10^7$ AGN in the survey and $\langle F_\alpha^2\rangle/\langle F_\alpha\rangle^2 \simeq 15$. We then find from Eq. (6),

$$\frac{S}{N} \simeq 5.7 f \left(\frac{(N_\nu/10^4)}{(\sigma/0.5°)(N_{\rm AGN}/2.8\times10^7)}\right)^{1/2} \times \left(\frac{\langle F_\alpha^2\rangle/\langle F_\alpha\rangle^2}{15}\right)^{1/2}\left(\frac{f_{\rm sky}}{0.5}\right)^{1/2}. \quad (11)$$

B. Angular information and timing

With our models for AGN variability and the AGN luminosity/redshift distribution, we infer an rms fractional flux variation of $\langle\sigma_{\rm var}^2\rangle \simeq 0.54$. The estimate in Eq. (11) is thus enhanced by approximately 12%.

This calculation can also be understood in a different way. It suggests that if AGN are determined from angular information to contribute a fraction f of the observed neutrinos, then a correspondence between instantaneous AGN luminosity and neutrino luminosity can be established with a signal-to-noise of $[\langle\sigma_{\rm var}^2\rangle/2]^{1/2}$ times the value in Eq. (11).

C. IceCube, KM3NET, and Baikal-GVD

We now present numerical results including the sky-averaged effective areas for IceCube, KM3NET, and Baikal-GVD for the regions of sky that overlap with those surveyed by Rubin—to a first approximation, though, they are all comparable. We take the angular resolution of IceCube to be 0.5° and those for KM3NET and Baikal-GVD to be 0.2°. The total exposure time is taken to be 10 years. We plot the signal-to-noise ratio from angular information alone, from timing, and from the total, in Fig. 5. The green curve there shows the signal-to-noise for a measurement where f is inferred only from a correlation of the neutrino arrival time with AGN variability, assuming our canonical value for $\langle F^2\rangle/\langle F\rangle^2$.

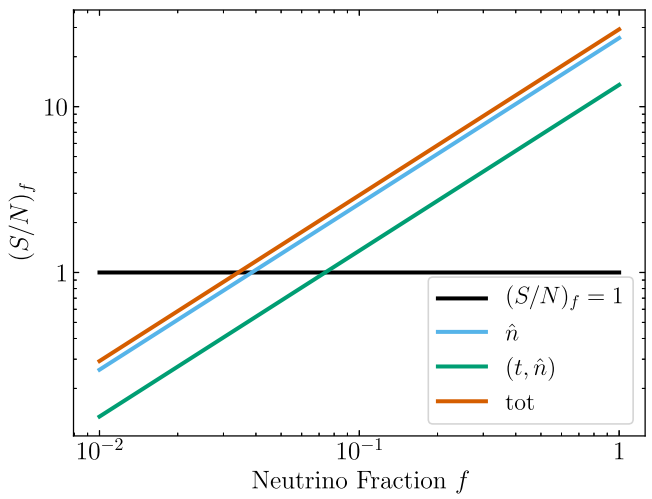

FIG. 5. The signal-to-noise ratio $(S/N)_f$ for measuring the HEAN neutrino fraction f using both temporal and spatial data from Rubin's *i* band, IceCube, KM3NeT, and Baikal-GVD. Since pure spatial correlation dominates the signal-to-noise ratio, the result is not very sensitive to the underlying AGN variability parameters. IceCube contributes ∼8% of the total signal-to-noise ratio, while KM3NeT and Baikal-GVD each give ∼46%.

V. DISCUSSION

We clarify four assumptions and present three comments. First, our main assumption is linearity between neutrino number and AGN bolometric luminosity. Even if linearity holds true, various AGN may have different proportionality constants due to some additional specification of AGN class (e.g., this scenario already occurs with redshift). This will then be encoded in a change to $\langle F^2\rangle/\langle F\rangle^2$. Additional classes in the variability properties will change the value of $\langle\sigma_{\rm var}^2\rangle$ relative to the value obtained in our canonical model. It is also possible that the number of neutrinos is not linear in the AGN's bolometric luminosity, but some power γ, with $0 \le \gamma \le 2$ [10]. We leave the investigation of both these cases for future work.

Second, we chose a specific form (the damped random walk) for the intensity autocorrelation function for AGN. This form, while applicable to a majority of AGN, has some exceptions. Changes in the slope, break, as well additional slopes and breaks, are all required to encapsulate a greater range of AGN morphologies. However, for our forecast analysis, such changes will only result in a rescaling of the scaled variance $\langle F^2\rangle/\langle F\rangle^2$. In particular, if the change in the variability properties shifts the variability timescales outside of the measurable window allowed by the Rubin cadence, then the prospects to detect a neutrino-AGN temporal correlation will decrease, while if more power is concentrated in this window, they may become stronger.

Third, we set the time delay between the neutrino signal and AGN variability to zero. This was done for simplicity, and in reality there should be an expected delay depending on where within the AGN the neutrino was created and where the variability is sourced. We leave formalizing this description for future work.

Fourth, we assumed that neutrinos travel along the line of sight unimpeded. The presence of neutrino self-interactions [64] can change this description, altering the spatial and temporal coincidence presented here [65,66]. We also leave exploration of this scenario for future work.

In our analysis, we consider cross-correlating the entire Rubin catalog with several high-energy neutrino maps. Cross-correlating only a subpopulation of the Rubin catalog, instead, could yield a higher signal-to-noise, as given by our estimation in Eq. (6). If possible, certain subpopulations would then be able to be detected or ruled out as definitive sources at higher significance. It is worth noting, however, that for a given source model of high-energy neutrino production the expected signal also decreases with a smaller subpopulation (if that smaller population removes sources in the model of interest).

Therefore, reducing the number of AGN in a cross-correlation study will not always yield more promising results. Regardless, we have shown here that, even without maximizing the signal-to-noise for a given source model, future AGN/neutrino cross-correlations will still be able to detect signals even if the Rubin catalog only contributes to a tenth of the entire HEAN flux.

Measurements of the neutrino fraction f have covariance with measurements of AGN variability parameters. Therefore, in principle the error in measurements of f should be larger than that presented here. However, given Rubin's precise measurements of an AGN's variability parameters, we expect such degradation of measurement fidelity to be slight and our forecast to hold.

Finally, we choose to neglect energy dependence in our analysis in order obtain conservative sensitivity estimates that are model-independent. In general, it is expected that sources with a harder spectrum are easier to detect, and prior work shows that inclusion of such model dependency improves the sensitivity by a factor of ∼2 (depending on the source spectrum assumed) [50]. We expect that most of the AGN that will be detected by Rubin will be radio quiet.

VI. CONCLUSION

In this paper we investigated the prospects to detect an angular cross-correlation between AGN surveyed by Rubin and energetic neutrinos. We then discussed further the prospects to detect a cross-correlation between AGN variability and neutrino arrival times.

With this aim, we first modeled the spatial cross-correlation between a single AGN and a population of neutrinos and found a neutrino-counting measure. More specifically, the contributions to this correlation were from counting neutrinos sourced by that AGN and from counting neutrinos with other sources that have nonzero overlap with that AGN due to angular error.

AGN may emit electromagnetic radiation along with HEANs, and to account for this possibility, we also modeled a temporal-and-spatial cross-correlation. For simplicity, we assumed that, for each AGN, the number of neutrinos emitted is proportional to the electromagnetic intensity of that AGN.

Using both of these correlations, we then forecasted their individual and total abilities to measure the fraction f of HEAN from Rubin-observed AGN. The HEANs are detected by a combination of IceCube, KM3NeT, and Bakail-GVD, and we assumed an IceCube-like sky-averaged effective area for each experiment. In accordance with previous work, we took all AGN in the Rubin sample to be measured with high signal-to-noise. We thus found that, given 10 years of observation time, temporal and spatial cross-correlations will be able to establish an association between energetic neutrinos and the AGN in Rubin even if such AGN contribute only ∼10% of the neutrino background. Finally, given that the background noise scales with $N_{\mathrm{AGN}}^{-1/2}$, it should be possible to establish a correlation between neutrinos and some specific subclass of AGN, even if those AGN contribute less than ∼10% of the neutrino background.

ACKNOWLEDGMENTS

C. C. S. acknowledges the support of the Bill and Melinda Gates Foundation. C. C. S. was supported by a National Science Foundation Graduate Research Fellowship under Grant No. DGE-1746891. This work was supported in part by the Simons Foundation and by National Science Foundation Grant No. 2112699.

APPENDIX: ASSUMPTION OF UNIFORM BACKGROUND

In this section, we justify that the assumption of uniform distribution for the background events (i.e., $B_i = (4\pi f_{\mathrm{sky}})^{-1}$) does not affect our forecasted sensitivity.

We simulate 5000 sources with their sky locations drawn from a uniform distribution on a 2D sphere. Then, following the procedures in Ref. [12], we calculate the limit/sensitivity that can be set by evaluating the maximum-likelihood estimator (Eq. (1)). The limit is calculated for two different cases. First is using IceCube's 10 years of data (track events) and the realistic background PDFs which are

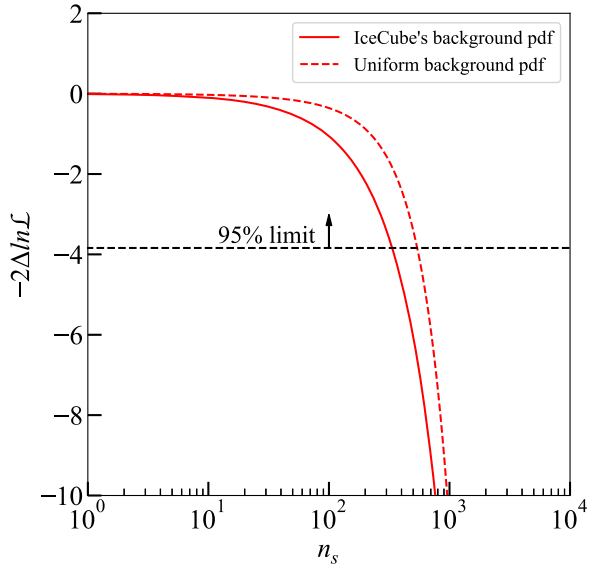

FIG. 6. Forecasted sensitivities to a catalog of simulated 5000 source from numerical calculations of the maximum-likelihood estimator (Eq. (1)). Solid line uses IceCube's 10 years of data and the corresponding background PDF. Dashed line uses the same number of simulated events with arrival directions drawn from uniform distributions of right ascension and cos(zenith angle) and the corresponding background PDF, $B_i = (4\pi f_{\mathrm{sky}})^{-1}$.

derived from the data [12]. The second is using the simulated data which consists of the same number of track events with arrival directions drawn from uniform distributions of right ascension and cos(zenith angle) and the corresponding background PDF, $B_i = (4\pi f_{\rm sky})^{-1}$. The 95% limit (sensitivity) is set by a deviation of $\ln\mathcal{L}$ from when $f = 0$ by 3.84, i.e., $\Delta\ln\mathcal{L} = -3.84$. Note that $f = 0$ means all the events come from the background.

Figure 6 shows the result. The likelihood curves are close for the two cases and the 95% upper limits on n_s are within a factor of two, where $n_s = f \times N_\nu$ is the total number of neutrinos coming from the sources.

[1] J. Stettner (IceCube Collaboration), Measurement of the diffuse astrophysical muon-neutrino spectrum with ten tears of IceCube data, Proc. Sci., ICRC2019 (**2020**) 1017 .

[2] M. G. Aartsen *et al.* (IceCube Collaboration), Characteristics of the Diffuse Astrophysical Electron and Tau Neutrino Flux with Six Years of IceCube High Energy Cascade Data, Phys. Rev. Lett. **125**, 121104 (2020).

[3] R. Abbasi *et al.* (IceCube Collaboration), The IceCube high-energy starting event sample: Description and flux characterization with 7.5 years of data, Phys. Rev. D **104**, 022002 (2021).

[4] R. Abbasi *et al.* (IceCube Collaboration), IceCube Data for Neutrino Point-Source Searches Years 2008-2018, arXiv: 2101.09836.

[5] M. G. Aartsen *et al.* (IceCube Collaboration), Neutrino emission from the direction of the blazar TXS 0506 + 056 prior to the IceCube-170922A alert, Science **361**, 147 (2018).

[6] M. G. Aartsen *et al.* (IceCube, Fermi-LAT, MAGIC, AGILE, ASAS-SN, HAWC, H.E.S.S., INTEGRAL, Kanata, Kiso, Kapteyn, Liverpool Telescope, Subaru, Swift NuSTAR, VERITAS and VLA/17B-403 Collaborations), Multimessenger observations of a flaring blazar coincident with high-energy neutrino IceCube-170922A, Science **361**, eaat1378 (2018).

[7] T. Glüsenkamp (IceCube Collaboration), Analysis of the cumulative neutrino flux from Fermi-LAT blazar populations using 3 years of IceCube data, EPJ Web Conf. **121**, 05006 (2016).

[8] A. Palladino and F. Vissani, Can BL Lacertae emission explain the neutrinos above 0.2 PeV?, Astron. Astrophys. **604**, A18 (2017).

[9] K. Murase, F. Oikonomou, and M. Petropoulou, Blazar flares as an origin of high-energy cosmic neutrinos?, Astrophys. J. **865**, 124 (2018).

[10] C. Yuan, K. Murase, and P. Mészáros, Complementarity of stacking and multiplet constraints on the blazar contribution to the cumulative high-energy neutrino intensity, Astrophys. J. **890**, 25 (2020).

[11] D. Smith, D. Hooper, and A. Vieregg, Revisiting AGN as the source of IceCube's diffuse neutrino flux, J. Cosmol. Astropart. Phys. 03 (2021) 031.

[12] B. Zhou, M. Kamionkowski, and Y. f. Liang, Search for high-energy neutrino emission from radio-bright AGN, Phys. Rev. D **103**, 123018 (2021).

[13] P. A. Abell *et al.* (LSST Science and LSST Project Collaborations), LSST Science Book, Version 2.0, arXiv: 0912.0201.

[14] S. Adrian-Martinez *et al.* (KM3Net Collaboration), Letter of intent for KM3NeT 2.0, J. Phys. G **43**, 084001 (2016).

[15] A. D. Avrorin *et al.* (Baikal-GVD Collaboration), Baikal-GVD: Status and prospects, EPJ Web Conf. **191**, 01006 (2018).

[16] K. Murase, M. Ahlers, and B. C. Lacki, Testing the hadronuclear origin of PeV neutrinos observed with IceCube, Phys. Rev. D **88**, 121301 (2013).

[17] R. Y. Liu, K. Wang, R. Xue, A. M. Taylor, X. Y. Wang, Z. Li, and H. Yan, Hadronuclear interpretation of a high-energy neutrino event coincident with a blazar flare, Phys. Rev. D **99**, 063008 (2019).

[18] J. P. Rachen and P. Meszaros, Photohadronic neutrinos from transients in astrophysical sources, Phys. Rev. D **58**, 123005 (1998).

[19] W. Winter, Photohadronic origin of the TeV-PeV neutrinos observed in IceCube, Phys. Rev. D **88**, 083007 (2013).

[20] J. C. Rodríguez-Ramírez, E. M. de Gouveia Dal Pino, and R. Alves Batista, Very-high-energy emission from magnetic reconnection in the radiative-inefficient accretion flow of SgrA, Astrophys. J. **879**, 6 (2019).

[21] T. Inoue, Bell-instability-mediated spectral modulation of hadronic gamma rays from a supernova remnant interacting with a molecular cloud, Astrophys. J. **872**, 46 (2019).

[22] S. S. Kimura, K. Murase, and P. Mészáros, Soft gamma rays from low accreting supermassive black holes and connection to energetic neutrinos, Nat. Commun. **12**, 5615 (2021).

[23] K. Mannheim, High-energy neutrinos from extragalactic jets, Astropart. Phys. **3**, 295 (1995).

[24] K. Murase, Y. Inoue, and C. D. Dermer, Diffuse neutrino intensity from the inner jets of active galactic nuclei: Impacts of external photon fields and the blazar sequence, Phys. Rev. D **90**, 023007 (2014).

[25] F. Tavecchio, C. Righi, A. Capetti, P. Grandi, and G. Ghisellini, High-energy neutrinos from FR0 radio-galaxies?, Mon. Not. R. Astron. Soc. **475**, 5529 (2018).

[26] F. W. Stecker and M. H. Salamon, High-energy neutrinos from quasars, Space Sci. Rev. **75**, 341 (1996).

[27] K. Murase, S. S. Kimura, and P. Meszaros, Hidden Cores of Active Galactic Nuclei as the Origin of Medium-Energy Neutrinos: Critical Tests with the MeV Gamma-Ray Connection, Phys. Rev. Lett. **125**, 011101 (2020).

[28] Y. Inoue, D. Khangulyan, and A. Doi On the origin of high-energy neutrinos from NGC 1068: The role of nonthermal coronal activity, Astrophys. J. Lett. **891**, L33 (2020).

[29] E. M. Gutiérrez, F. L. Vieyro, and G. E. Romero, Nonthermal processes in hot accretion flows onto supermassive

black holes: An inhomogeneous model, Astron. Astrophys. **649**, A87 (2021).
[30] Y. Inoue, D. Khangulyan, and A. Doi, Gamma-ray and neutrino signals from accretion disk coronae of active galactic nuclei, Galaxies **9**, 36 (2021).
[31] N. Senno, K. Murase, and P. Meszaros, Choked jets and low-luminosity gamma-ray bursts as hidden neutrino sources, Phys. Rev. D **93**, 083003 (2016).
[32] K. Murase, S. S. Kimura, B. T. Zhang, F. Oikonomou, and M. Petropoulou, High-energy neutrino and gamma-ray emission from tidal disruption events, Astrophys. J. **902**, 108 (2020).
[33] N. Senno, K. Murase, and P. Mészáros, Constraining high-energy neutrino emission from choked jets in stripped-envelope supernovae, J. Cosmol. Astropart. Phys. 01 (2018) 025.
[34] A. Esmaili and K. Murase, Constraining high-energy neutrinos from choked-jet supernovae with IceCube high-energy starting events, J. Cosmol. Astropart. Phys. 12 (2018) 008.
[35] J. Necker *et al.* (IceCube Collaboration), Searching for high-energy neutrinos from core-collapse supernovae with IceCube, Proc. Sci., ICRC2021 (**2021**) 1116.
[36] V. Berezinsky, E. Sabancilar, and A. Vilenkin, Extremely high energy neutrinos from cosmic strings, Phys. Rev. D **84**, 085006 (2011).
[37] C. Lunardini and E. Sabancilar, Cosmic strings as emitters of extremely high energy neutrinos, Phys. Rev. D **86**, 085008 (2012).
[38] L. A. Anchordoqui, T. C. Paul, L. H. M. da Silva, D. F. Torres, and B. J. Vlcek, What IceCube data tell us about neutrino emission from star-forming galaxies (so far), Phys. Rev. D **89**, 127304 (2014).
[39] P. Padovani and E. Resconi, Are both BL Lacs and pulsar wind nebulae the astrophysical counterparts of IceCube neutrino events?, Mon. Not. R. Astron. Soc. **443**, 474 (2014).
[40] S. Sahu and L. S. Miranda, Some possible sources of IceCube TeV–PeV neutrino events, Eur. Phys. J. C **75**, 273 (2015).
[41] R. Moharana and S. Razzaque, Angular correlation of cosmic neutrinos with ultrahigh-energy cosmic rays and implications for their sources, J. Cosmol. Astropart. Phys. 08 (2015) 014.
[42] K. Emig, C. Lunardini, and R. Windhorst, Do high energy astrophysical neutrinos trace star formation?, J. Cosmol. Astropart. Phys. 12 (2015) 029.
[43] S. Ando, I. Tamborra, and F. Zandanel, Tomographic Constraints on High-Energy Neutrinos of Hadronuclear Origin, Phys. Rev. Lett. **115**, 221101 (2015).
[44] M. G. Aartsen *et al.* (IceCube Collaboration), Time-Integrated Neutrino Source Searches with 10 Years of IceCube Data, Phys. Rev. Lett. **124**, 051103 (2020).
[45] A. Plavin, Y. Y. Kovalev, Y. A. Kovalev, and S. Troitsky, Observational evidence for the origin of high-energy neutrinos in parsec-scale nuclei of radio-bright active galaxies, Astrophys. J. **894**, 101 (2020).
[46] K. Fang, A. Banerjee, E. Charles, and Y. Omori, A cross-correlation study of high-energy neutrinos and tracers of large-scale structure, Astrophys. J. **894**, 112 (2020).
[47] R. Abbasi *et al.* (IceCube Collaboration), A search for neutrino emission from cores of Active Galactic Nuclei, arXiv:2111.10169.
[48] R. Abbasi *et al.* (IceCube Collaboration), Time-integrated searches for point-like sources of neutrinos with the 40-string IceCube detector, Astrophys. J. **732**, 18 (2011).
[49] M. G. Aartsen *et al.* (IceCube Collaboration), Search for time-independent neutrino emission from astrophysical sources with 3 yr of IceCube data, Astrophys. J. **779**, 132 (2013).
[50] J. Braun, J. Dumm, F. De Palma, C. Finley, A. Karle, and T. Montaruli, Methods for point source analysis in high energy neutrino telescopes, Astropart. Phys. **29**, 299 (2008).
[51] J. Braun, M. Baker, J. Dumm, C. Finley, A. Karle, and T. Montaruli, Time-dependent point source search methods in high energy neutrino astronomy, Astropart. Phys. **33**, 175 (2010).
[52] N. Aghanim *et al.* (Planck Collaboration), Planck 2018 results. VI. Cosmological parameters, Astron. Astrophys. **641**, A6 (2020); **652**, C4(E) (2021).
[53] P. F. Hopkins, G. T. Richards, and L. Hernquist, An observational determination of the bolometric quasar luminosity function, Astrophys. J. **654**, 731 (2007).
[54] C. Creque-Sarbinowski, M. Kamionkowski, and B. Zhou, AGN variability in the age of VRO, arXiv:2110.13149.
[55] C. L. MacLeod, Z. Ivezic, C. S. Kochanek, S. Kozlowski, B. Kelly, E. Bullock, A. Kimball, B. Sesar, D. Westman, K. Brooks *et al.*, Modeling the time variability of SDSS stripe 82 quasars as a damped random walk, Astrophys. J. **721**, 1014 (2010).
[56] C. L. MacLeod, Z. Ivezic, B. Sesar, W. de Vries, C. S. Kochanek, B. C. Kelly, A. C. Becker, R. H. Lupton, P. B. Hall, G. T. Richards *et al.*, A description of quasar variability measured using repeated SDSS and POSS imaging, Astrophys. J. **753**, 106 (2012).
[57] Y. Zu, C. S. Kochanek, S. Kozlowski, and A. Udalski, Is quasar variability a damped random walk?, Astrophys. J. **765**, 106 (2013).
[58] S. Kozłowski, A degeneracy in DRW modelling of AGN light curves, Mon. Not. R. Astron. Soc. **459**, 2787 (2016).
[59] S. Kozłowski, Limitations on the recovery of the true AGN variability parameters using damped random walk modeling, Astron. Astrophys. **597** (2017).
[60] S. Kozłowski, A method to measure the unbiased decorrelation timescale of the AGN variable signal from structure functions Astrophys. J. **835**.
[61] L. F. Sartori, B. Trakhtenbrot, K. Schawinski, N. Caplar, E. Treister, and C. Zhang, A forward modelling approach to AGN variability—Method description and early applications, Astrophys. J. **883**, 139 (2019).
[62] V. P. Kasliwal, M. S. Vogeley, and G. T. Richards, Extracting information from AGN variability, Mon. Not. R. Astron. Soc. **470**, 3027 (2017).
[63] C. J. Burke, Y. Shen, O. Blaes, C. F. Gammie, K. Horne, Y. F. Jiang, X. Liu, I. M. McHardy, C. W. Morgan,

S. Scaringi, and Q. Yang, A characteristic optical variability timescale in astrophysical accretion disks, Science **373**, 789 (2021).

[64] C. Creque-Sarbinowski, J. Hyde, and M. Kamionkowski, Resonant neutrino self-interactions, Phys. Rev. D **103**, 023527 (2021).

[65] S. Koren, Neutrino—dark matter scattering and coincident detections of UHE neutrinos with EM sources, J. Cosmol. Astropart. Phys. 09 (2019) 013.

[66] K. Murase and I. M. Shoemaker, Neutrino Echoes from Multimessenger Transient Sources, Phys. Rev. Lett. **123**, 241102 (2019).